

E7-2006-102

SEARCH FOR FUSION SUPPRESSION
IN REACTIONS HAVING ENTRANCE-CHANNEL
MASS-ASYMMETRY VALUES AROUND
THE BUSINARO–GALLONE POINT

Submitted to the 11th International Conference on Nuclear Reaction
Mechanisms, June 12–16, 2006, Villa Monastero, Varenna, Italy

R. N. Sagaidak, A. Yu. Chizhov, G. N. Kniajeva, M. G. Itkis,
N. A. Kondratiev, E. M. Kozulin, I. V. Pokrovsky
*Flerov Laboratory of Nuclear Reactions, JINR, 141980 Dubna,
Moscow region, Russia*

L. Corradi, E. Fioretto, A. Gadea, A. M. Stefanini
*INFN, Laboratori Nazionali di Legnaro, I-35020 Legnaro,
Padova, Italy*

S. Beghini, G. Montagnoli, F. Scarlassara
*Dipartimento di Fisica and INFN, Università di Padova,
I-35131 Padova, Italy*

M. Trotta
INFN, Sezione di Napoli, Napoli, Italy

S. Szilner
Ruder Bošković Institute, HR-10 002 Zagreb, Croatia

Сагайдак Р. Н. и др.

E7-2006-102

Поиск ограничений на слияние в реакциях, имеющих значения масс-асимметрии во входном канале вокруг точки Бусинаро–Галоне

Проведен анализ функций возбуждения для испарительных остатков и деления в рамках потенциальной модели слияния и стандартной статистической модели, описывающей девозбуждение компаунд-ядер, образующихся в результате слияния. Рассмотрены реакции, имеющие различное значение масс-асимметрии во входном канале, но приводящие к одному и тому же компаунд-ядру. Заметное подавление образования испарительных остатков в комбинациях с меньшей асимметрией, наблюдаемое при сравнении данных с данными для сильно асимметричных комбинаций, приводящих к одному и тому же компаунд-ядру, может быть объяснено в рамках жидкокапельной модели. Это подавление определяется наличием условного барьера, возникающего вдоль координаты масс-асимметрии (точки Бусинаро–Галоне), на пути от контактной конфигурации налетающего ядра и ядра-мишени к их полному слиянию, т.е. к образованию сферического компаунд-ядра. Предприняты попытки найти корреляции между извлеченными в результате анализа вероятностями слияния и масс-асимметрией во входном канале, делимостью компаунд-ядер и деформациями сливающихся ядер.

Работа выполнена в Лаборатории ядерных реакций им. Г. Н. Флерова ОИЯИ.
Препринт Объединенного института ядерных исследований. Дубна, 2006

Sagaidak R. N. et al.

E7-2006-102

Search for Fusion Suppression in Reactions Having Entrance-Channel Mass-Asymmetry Values Around the Businaro–Gallone Point

Excitation functions for the evaporation residue (ER) production and fission have been analyzed in the framework of the potential barrier fusion model and standard statistical model describing the deexcitation of compound nuclei resulted in fusion. Reactions with a different entrance-channel mass-asymmetry, which lead to the same compound nucleus (CN) were considered. A pronounced suppression of the ER production in less asymmetric combinations, which is observed in comparison of the data with those obtained for very asymmetric ones leading to the same CN, could be explained in the framework of liquid-drop model considerations. It is determined by a presence of the conditional barrier along the mass-asymmetry coordinate (Businaro–Gallone point) on the path from a contact configuration of projectile and target nuclei to their complete fusion, i. e., to the spherical CN formation. Correlations between the values of the fusion probability derived in the analysis and the entrance-channel mass-asymmetry, CN fissility and deformations of fusing nuclei have been searched through the study.

The investigation has been performed at the Flerov Laboratory of Nuclear Reactions, JINR.

Preprint of the Joint Institute for Nuclear Research. Dubna, 2006

INTRODUCTION AND MOTIVATION

The production of heavy evaporation residues (ERs) in complete fusion reactions demonstrates a visible entrance channel effect of fusion suppression observed in quite asymmetric combinations with ^{19}F and ^{30}Si leading to the $^{216}\text{Ra}^*$ compound nucleus (CN). This statement follows from the comparison of the corresponding ER cross sections with those obtained in the $^{12}\text{C} + ^{204}\text{Pb}$ reaction leading to the same CN [1]. Such a fusion suppression is quite unexpected, especially for the reaction induced by ^{19}F , since the quasi-fission (QF) effect, which seems to be responsible for the lowering the ER production cross section, appears in reactions with Mg and heavier projectiles, as follows from the fission reaction studies [2, 3]. These observations motivated a further study of the entrance-channel effect at LNL (Legnaro), where we explored the less asymmetric combinations with ^{48}Ca leading to the $^{216,218}\text{Ra}^*$ and $^{202}\text{Pb}^*$ compound nuclei [4–6].

Our analysis of the measured excitation functions for ERs and fission [1, 5, 6] was performed within the framework of the potential barrier-passing model with the fluctuating barrier allowing to reproduce the effect of coupling the entrance channel to the other reaction channels [7]. The model treats the experimental capture cross section as the barrier-passing (BP) one. In the case of the analysis of measured fusion cross sections, it is usually assumed that all the partial waves passing through the barrier lead to fusion, i. e., the CN formation probability $P_{\text{CN}} = 1$. The standard statistical model (SSM) was used to describe the deexcitation of a CN resulted from the complete fusion of the projectile and target nuclei. Both models are incorporated into the HIVAP code [8]. In the analysis all the BP model parameters were fixed with the exception of the strength V_0 and the barrier fluctuation determined by the radius-parameter fluctuation $\sigma(r_0)/r_0$ in the exponential form of the nuclear potential [7]. Some variations of these parameters allowed us to achieve good agreement with the experimental data for fission and ER production at subbarrier energies. For strongly fissile compound nuclei, the ER cross sections at energies well above the Coulomb (Bass [9]) barrier are weakly sensitive to the form of the nuclear potential and are mainly determined by the SSM parameters. In use of SSM for the macroscopic level density parameters \tilde{a}_f and \tilde{a}_ν in the fission and evaporation channels, respectively, we chose the expression of W. Reisdorf [8]. The scaling factor k_f at the rotating liquid

drop (LD) fission barriers [10] in the expression for the shell corrected fission barriers $B_f(\ell) = k_f B_f^{LD}(\ell) - \Delta W_{gs}$ was used as a main fitted parameter in our analysis of the ER and fission cross sections. We fitted the excitation functions varying mainly k_f for the most asymmetric combinations such as C + Pb. We assumed an absence of any fusion suppression ($P_{CN} = 1$) in these cases and derived the fusion probability values for less asymmetric combinations using the same values of fission barriers and other parameters of the statistical model. We obtained the same fusion probability values $P_{CN} = 0.65$ and 0.55 for the ^{19}F - and ^{30}Si -induced reactions, respectively, as in [1] and lower values (~ 0.3) in the cases of $^{48}\text{Ca} + ^{168,170}\text{Er}$ [5]. Details are given in [5, 11].

The explanation of the fusion suppression effect was proposed in [1], in the framework of the LD model. It is suggested that the transition from the contact configuration to the CN configuration is determined by a presence of the conditional barrier along the mass-asymmetry coordinate [12] and the entrance-point

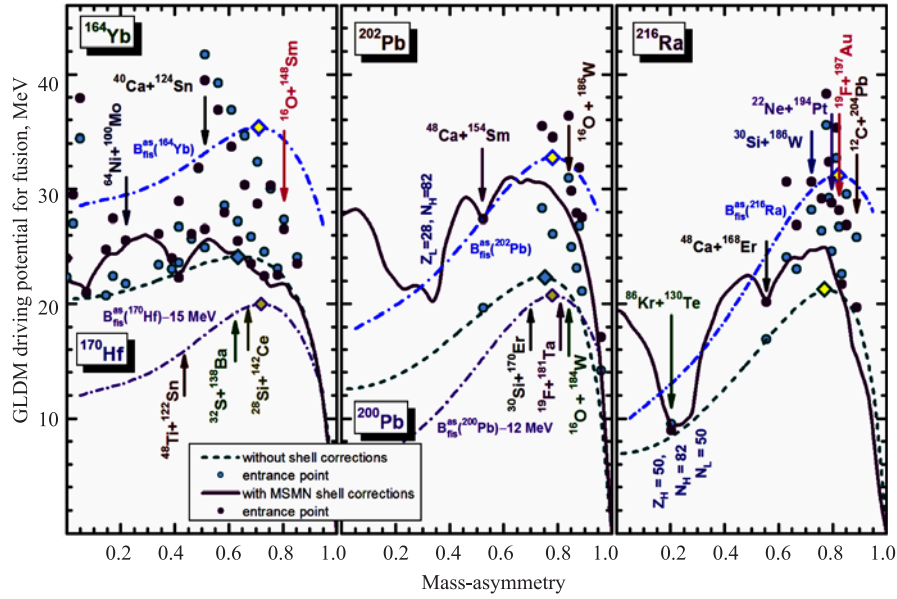


Fig. 1. Asymmetric LD fission barriers (dash-dotted lines) and driving potentials (solid and dashed lines) of the PES obtained in the framework of GLDM [14, 15] for non-fissile to fissile compound nuclei considered in the present study are plotted as a function of the mass-asymmetry. Arrows mark values of the entrance-channel mass-asymmetry for the combinations analyzed in this work; circles correspond to the PES calculations for the entrance-point asymmetry of available projectile-target combinations and diamonds — to the BG points

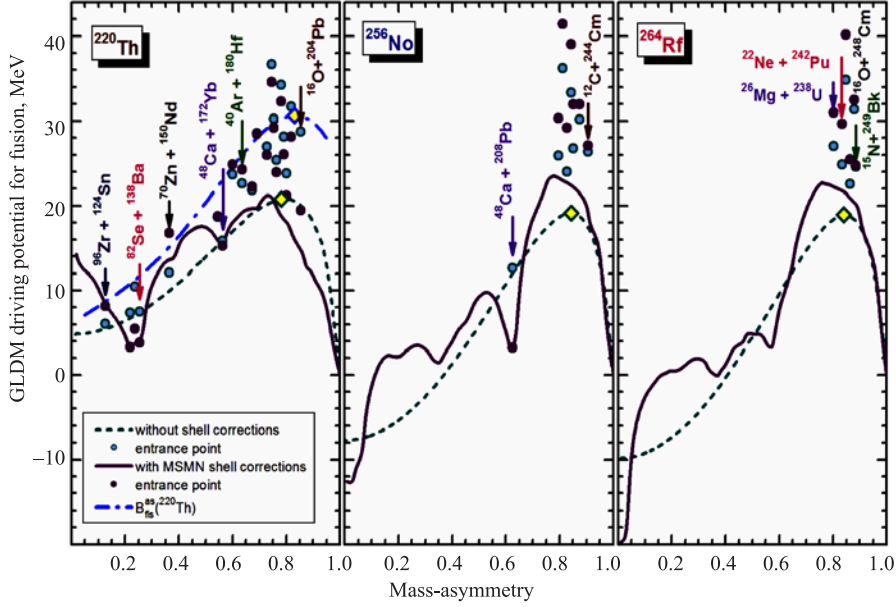


Fig. 2. The same as in Fig. 1, but for strongly fissile compound nuclei

position with respect to the top of the barrier, i.e., relatively to the Businaro–Gallone (BG) point [13]. Extrapolations of the calculations [12] show that the mass-asymmetry value for the $^{19}\text{F} + ^{197}\text{Au}$ combination corresponds to the vicinity of the BG point [1]. Calculations in the framework of the Generalized Liquid-Drop Model (GLDM) [14] give us a similar behavior of the asymmetric fission barriers. The BG point corresponds to the asymmetry, which can be realized in the $\text{Ne} + \text{Pt}$ and $\text{F} + \text{Au}$ reactions. Calculations of the potential energy surface (PES) in the (Z, N) -plane for the contact configuration of the projectile-target nuclei, with the use of the expression for the proximity energy [15], show a picture different from this one given by the asymmetric fission-barrier calculations [14]. The entrance points for asymmetric combinations (with Ar and lighter projectiles) leading to $^{216}\text{Ra}^*$ lay well above the bottom of the valley (the driving potential), on mountainsides of the PES. Shell corrections [16] strongly modulate the PES and the driving potential. In the framework of this approach fusion with ^{48}Ca and ^{86}Kr could be considered as the suppressed one, since their entrance points lay on the bottom of the valley (see the right panel in Fig. 1).

Of interest is a search for correlation between the entrance-channel mass-asymmetry and fusion probability for compound nuclei of different masses or fissility parameters. Of the same interest is disclosing the conditions when the

fusion suppression is starting to appear. In this paper we present the results of our analysis of the ER and fission excitation functions obtained in reactions with the different entrance-channel mass-asymmetry leading to the same compound nuclei. This work is a continuation of our previous work [11]. In the present study, we extend our analysis to non- (weakly-) fissile and strongly fissile (transuranium) compound nuclei. In Figs. 1 and 2 we indicate the corresponding entrance-channel mass-asymmetry values for the reactions, which have been analyzed in the present work and earlier [11], on plots of the BG family of the asymmetric fission barriers and driving potentials shown as a function of the mass-asymmetry.

The study of the entrance-channel effects in the production of compound nuclei of various masses (fissility) should help us to understand better the process of fusion in massive projectile-target combinations. It seems to be important from the point of view of the understanding of mechanisms of reactions used for the synthesis of superheavy nuclei.

RESULTS OF ANALYSIS AND DISCUSSION

The analysis of the ER excitation functions obtained for the reactions leading to the non- (weakly-) fissile $^{164}\text{Yb}^*$ CN [17–21] shows that calculations corresponding to the excitation energies below 50 MeV are rather insensitive to the magnitude of the LD barriers (see Fig. 3). The data are well reproduced with an adjustment of parameter values of the nuclear potential only. At the same time, in order to describe the ER cross sections at the excitation energies above 60 MeV for $^{40}\text{Ca} + ^{124}\text{Sn}$ [19] and for $^{64}\text{Ni} + ^{100}\text{Mo}$ [21], strongly reduced LD fission barriers ($k_f = 0.6$) are required that may denote some suppression of fusion. In that case, fission cross-section measurements can clarify the situation as well as ER cross-section measurements at the excitation energies above 70 MeV.

So, the present analysis of the available data does not allow us to say anything undoubtedly about the entrance-channel mass-asymmetry effect in the case of the ^{40}Ca - and ^{64}Ni -induced reactions leading to the $^{164}\text{Yb}^*$ CN. It should be noted that comparative analysis of the $^{164}\text{Yb}^*$ CN deexcitation at $E_{\text{CN}}^* \approx 54$ MeV has not revealed any entrance channel effects. It was concluded that the initial population of the CN is the only reason for the observed differences in the decay of $^{164}\text{Yb}^*$ populated in the $^{16}\text{O} + ^{148}\text{Sm}$ and $^{64}\text{Ni} + ^{100}\text{Mo}$ reactions [18]. The GLDM considerations indicate a presence of the noticeable asymmetric fission barrier on the way to fusion; whereas a position of the entrance point with respect to the driving potential (shell corrected and without shell corrections) does not suggest any hindrance for fusion at least for the ^{40}Ca -induced reaction (see the left panel in Fig. 1).

The analysis of the ER and fission excitation functions obtained in reactions leading to the weakly fissile $^{170}\text{Hf}^*\text{CN}$ [22, 23] again gives us rather uncertain

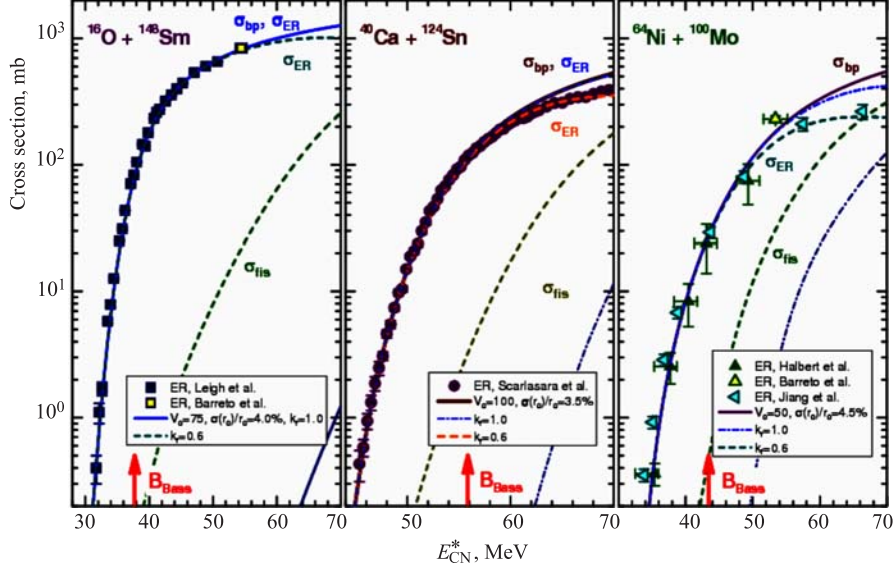


Fig. 3. ER excitation functions (sum of all measured evaporation channels) obtained in the $^{16}\text{O} + ^{148}\text{Sm}$ [17, 18], $^{40}\text{Ca} + ^{124}\text{Sn}$ [19] and $^{64}\text{Ni} + ^{100}\text{Mo}$ [18, 20, 21] reactions (symbols) leading to the $^{164}\text{Yb}^*$ CN in comparison with those calculated with HIVAP [7, 8] (lines)

results (see Fig. 4). Indeed the fission cross-section calculations show lowering the k_f -value in going from the ^{32}S - to ^{48}Ti -induced reactions that may denote some suppression. At the same time, the absence of the cross section data for a more asymmetric combination at high excitation energies does not allow us to state it surely.

For the moderately fissile $^{200}\text{Pb}^*\text{CN}$ no suppression has been revealed in the ^{19}F - and ^{30}Si -induced reactions according to our comparison of the ER and fission excitation functions measured in these reactions [24, 25] with those obtained in the ^{16}O -induced one [26]. It was shown in our analysis of the data [24–26] with HIVAP, which was performed earlier [11]. At the same time, in the reaction of ^{48}Ca with ^{154}Sm , we observe a significant fusion suppression corresponding to $P_{\text{CN}} \approx 0.6$, as follows from our comparison of the ER and fission cross sections [11, 27] with those obtained in the very asymmetric $^{16}\text{O} + ^{186}\text{W}$ reaction [26] leading to the same $^{202}\text{Pb}^*\text{CN}$.

For strongly fissile Th compound nuclei we started with the analysis of the excitation functions obtained in the $^{16}\text{O} + ^{208}\text{Pb}$ reaction [28–31] in order to extract parameter values of the nuclear potential and then to apply them to the

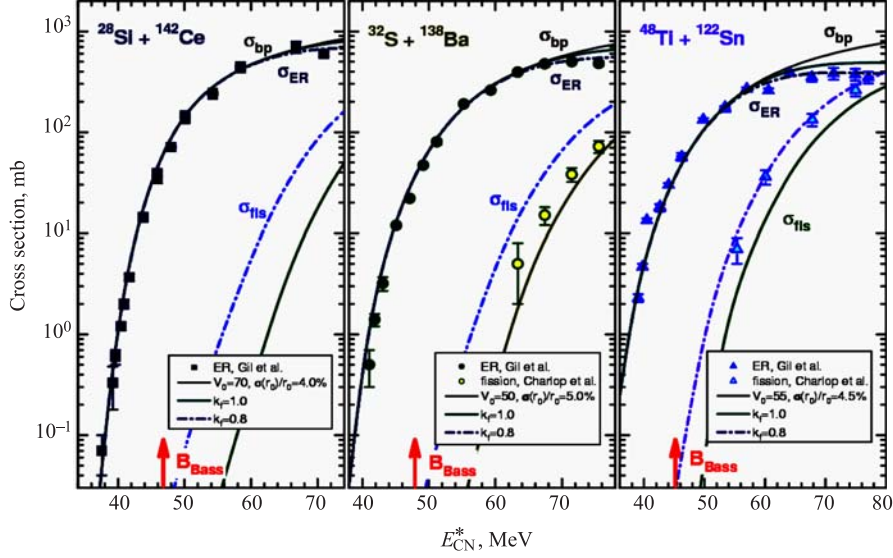


Fig. 4. ER and fission excitation functions obtained in the $^{28}\text{Si} + ^{142}\text{Ce}$ [22], $^{32}\text{S} + ^{138}\text{Ba}$ [22, 23] and $^{48}\text{Ti} + ^{122}\text{Sn}$ [22, 23] reactions (symbols) leading to the $^{170}\text{Hf}^*$ CN in comparison with those calculated with HIVAP (lines)

ER data obtained in $^{16}\text{O} + ^{204}\text{Pb}$ [32] leading to the $^{220}\text{Th}^*$ CN. We reproduced the excitation function [32] with a lower $k_f = 0.68$ value than in the case of $^{16}\text{O} + ^{208}\text{Pb}$ ($k_f = 0.78$) leading to $^{224}\text{Th}^*$. For $^{218,220}\text{Th}^*$, a number of ER excitation functions obtained in combinations with a different entrance-channel mass-asymmetry are available from literature. They can be reproduced only with the phenomenological introduction of $P_{\text{CN}} < 1$ in the framework of our analysis with HIVAP. The results for reactions leading to $^{220}\text{Th}^*$ were presented earlier [11, 33]. For the analysis of reactions leading to $^{218}\text{Th}^*$, we rescaled LD fission barriers obtained in our analysis of $^{16}\text{O} + ^{204}\text{Pb}$ using the $^{40}\text{Ar} + ^{178,180}\text{Hf}$ data [34, 35]. We used the rescaled $k_f = 0.64$ value in the analysis of the ER excitation functions obtained in more symmetric combinations. The results are shown in Fig. 5. In order to reproduce some excitation functions at subbarrier energies, e. g., $^{70}\text{Zn} + ^{150}\text{Nd}$ [36], $^{58}\text{Fe} + ^{160}\text{Gd}$ [37] and $^{64}\text{Ni} + ^{154}\text{Sm}$ [38], the extra-extra push energy parameterized as in [3] should be added to the fusion barrier. All these cases relate to the reactions with strongly deformed target nuclei. In fact, such results imply that only «side» or short radius collisions corresponding to higher fusion barriers lead mainly to fusion following with the ER production, whereas «tip» or long radius collisions may result in QF without ER production.

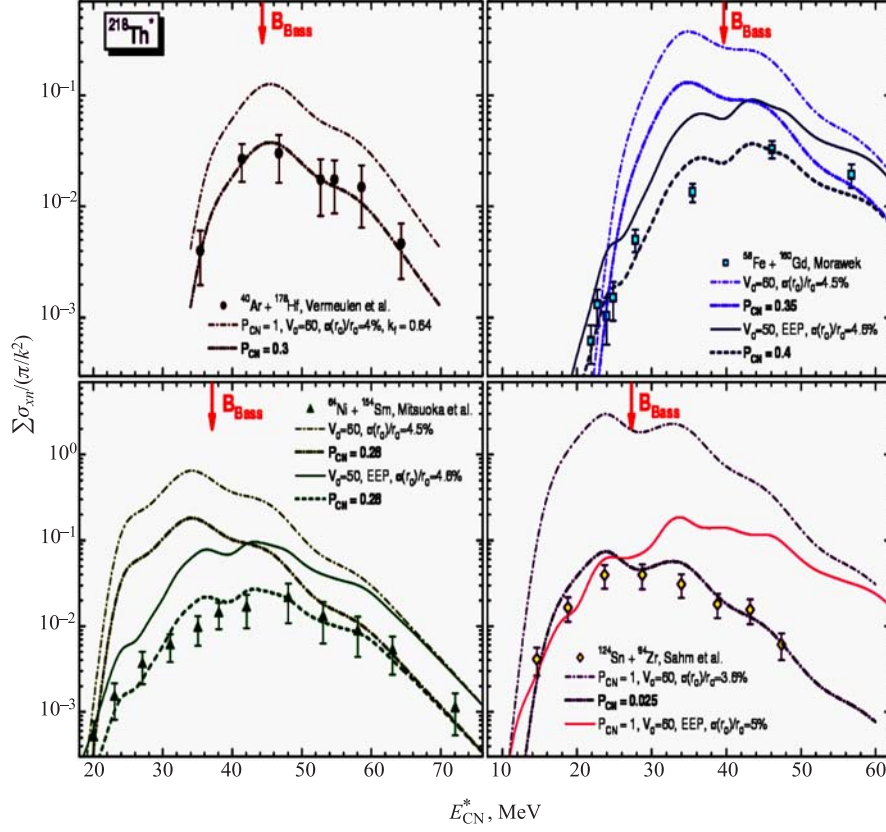


Fig. 5. The reduced cross sections for ERs produced in xn -evaporation channels in reactions leading to $^{218}\text{Th}^*$ [34, 37–39] in comparison with those calculated with HIVAP using $P_{\text{CN}} = 1$ and the P_{CN} values adjusted to reproduce the experimental data (lines)

The QF effect connected with the target nucleus deformation is clearly manifested at subbarrier energies in the very asymmetric $^{16}\text{O} + ^{238}\text{U}$ combination leading to the formation of strongly fissile $^{254}\text{Fm}^*$. As we see in Fig. 6, fission and ER excitation functions obtained in [40–42] can be described with the different values of the fusion-barrier fluctuation parameter $\sigma(r_0)/r_0$. It means that the extra-fission cross sections obtained below the fusion barrier [9] correspond mainly to the QF ones. This statement is in agreement with the results of the analysis of the fission-fragment angular anisotropy [40]. It is remarkable that we used 18–20% higher than nominal LD fission barriers [10] in order to describe the excitation functions for the production of the relatively neutron-rich Fm nuclei

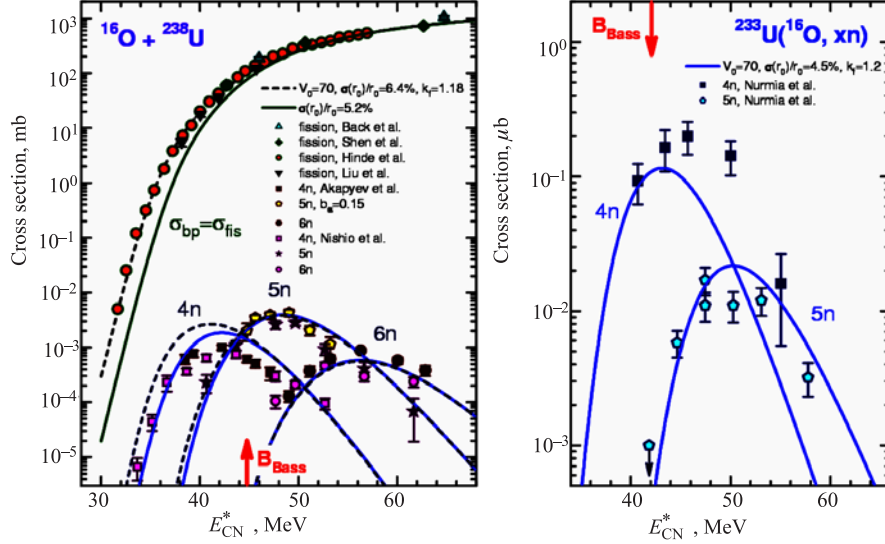


Fig. 6. The results of our analysis with HIVAP [7, 8] (lines) of the ER and fission excitation functions obtained in the $^{16}\text{O} + ^{238}\text{U}$ reaction [40–42] leading to $^{254}\text{Fm}^*$ (left panel) and the ER excitation functions obtained in the $^{16}\text{O} + ^{233}\text{U}$ reaction [43] leading to $^{249}\text{Fm}^*$ (right panel)

as well as the neutron-deficient ones. The last were produced in the reaction with ^{233}U [43] (see Fig. 6). Similarly, we had to use 20% higher than nominal LD fission barriers in order to describe the excitation functions for the production of No nuclei in the C + Cm reactions [44].

Applying these results to the production of the Fm isotopes in the cold fusion reaction with ^{40}Ar , we had to introduce phenomenologically the 10% fusion probability in order to describe the measured ER excitation functions [45]. The alternative independent fit to the ER data gives us significantly smaller LD fission barriers ($k_f = 0.9$) that contradicts to the results of our analysis of the asymmetric reactions with ^{16}O . The derived value of $P_{\text{CN}} = 0.1$ is below the value for the CN fission, i. e., fusion, which was obtained with the analysis of the fission-fragment charge-angular distributions measured in the same reaction [46] (see Fig. 7). One should mention that this estimate of the CN-fission contribution was derived without any selection of the total kinetic energy of fragments and its variance for the observed fission (fission-like) events. Comparing the ER cross sections measured in the $^{48}\text{Ca} + ^{208}\text{Pb}$ reaction [47–50] with those obtained in $^{12}\text{C} + ^{244}\text{Cm}$ [44] leading to the same $^{256}\text{No}^*$ CN, very similar results are obtained in the analysis of the excitation functions for the former. The value of $P_{\text{CN}} = 0.15$

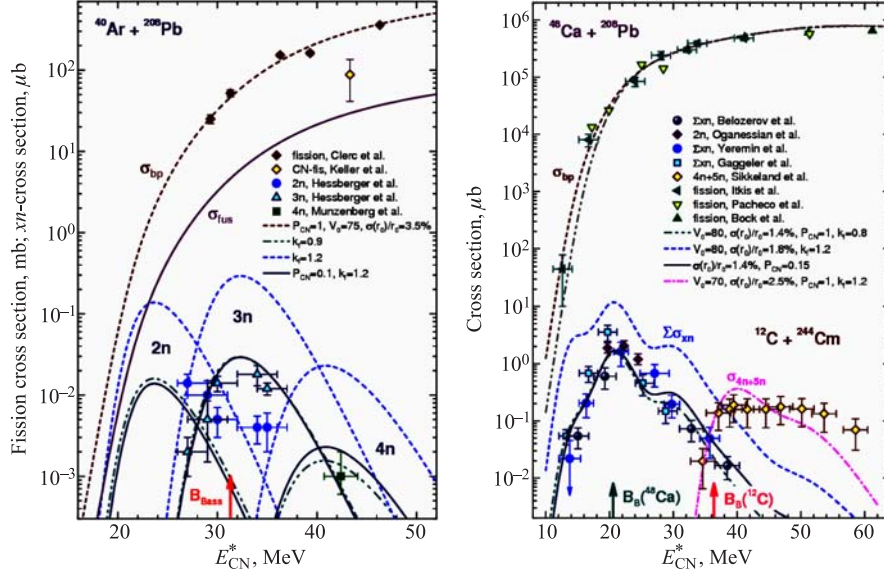


Fig. 7. The results of our analysis with HIVAP [7, 8] (lines) of the ER and fission excitation functions obtained for the cold fusion reactions: $^{40}\text{Ar} + ^{208}\text{Pb}$ [35, 45, 46] leading to $^{248}\text{Fm}^*$ (left panel); and $^{48}\text{Ca} + ^{208}\text{Pb}$ [47–53], which is compared with $^{12}\text{C} + ^{244}\text{Cm}$ [44] (both lead to the same $^{256}\text{No}^*$ CN) (right panel)

is derived with the same LD fission barriers as obtained in our analysis of the xn -excitation functions obtained in the C + Cm reactions (see above) leading to the production of No isotopes with various atomic mass numbers [44]. Again, the alternative independent fit to the ER data gives us significantly smaller LD fission barriers ($k_f = 0.8$) that contradicts to the results of our analysis of the asymmetric C + Cm reactions (see Fig. 7).

The analysis of the very asymmetric hot fusion reactions with ^{15}N and ^{16}O leading to $^{264}\text{Rf}^*$ [54, 55] shows that we should use again 20% higher than nominal LD fission barriers in order to reproduce the measured xn -excitation functions. Applying this result to the data obtained in less asymmetric combinations with ^{22}Ne and ^{26}Mg , we have to introduce the 50% fusion probability to describe the xn cross sections obtained in these cases [56]. The value of $P_{\text{CN}} = 0.5$ corresponds to the fusion cross sections deduced from the fission study in the $^{26}\text{Mg} + ^{238}\text{U}$ reaction [3] (see Fig. 8).

Of partial interest is an estimate of the fusion probability for asymmetric reactions with ^{48}Ca leading to the formation of the compound nuclei close to the island of stability of the superheavies reaching around the most stable one with

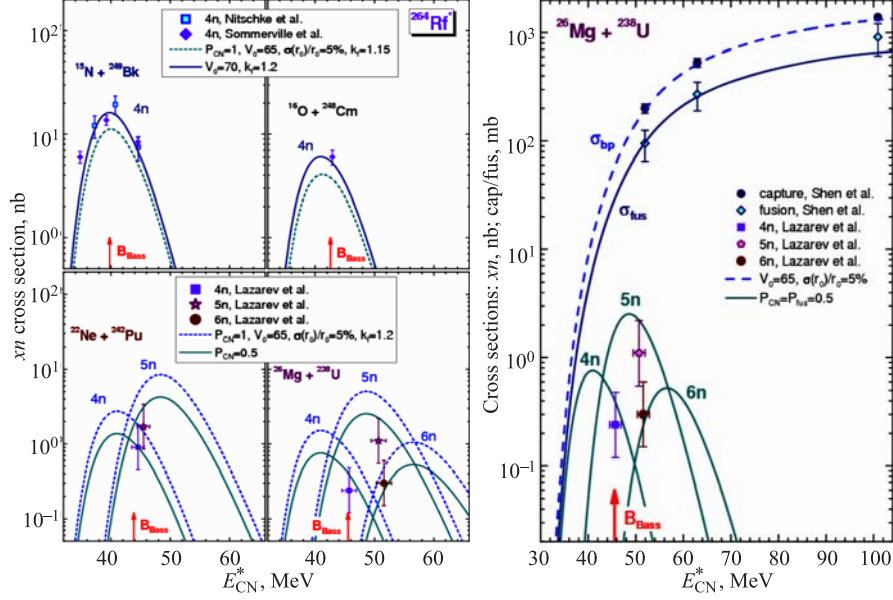


Fig. 8. The results of our analysis of xn -excitation functions obtained for asymmetric hot fusion reactions leading to $^{264}\text{Rf}^*$ [54–56] (upper left panels) and their application to the results of fission study in $^{26}\text{Mg} + ^{238}\text{U}$ [3] (right panel)

$Z = 114$ and $N = 184$. Survivability of such nuclei having a zero LD barrier is mainly determined by the shell corrections to the barriers. This circumstance simplifies the analysis, since we do not need anymore to vary k_f at the LD barriers. Bearing in mind the available data on fission [3, 53] and ER production [57], we chose the $^{48}\text{Ca} + ^{238}\text{U}$ reaction for the analysis. Unfortunately, the fission data sets are not in agreement with each other and, consequently, two quite different fusion probability functions could be derived from the data [3, 53]. We could not reproduce the ER data, fitting the capture cross sections measured in fission experiments with the calculated barrier passing ones and applying the fusion probability functions derived from the same experiments to the calculated ER excitation functions. The data [3] give us the ER excitation function with the maximum laying well below the nominal fusion barrier energy [9] that is not observed in the ^{48}Ca experiments with actinide targets [57, 58]. The data [53] lead to the calculated ER excitation function with the position of maximum close to the one observed in the experiment, but the absolute cross section values are about an order of magnitude higher than those obtained in [57]. In this case, we derived the fusion probability value as a ratio of the maximal ER cross section measured in [57] to the calculated one at the same excitation energy.

Attempting to search out scaling for the fusion probability values derived in our analysis, we have plotted them as a function of the entrance-channel mass-asymmetry (see Fig. 9). As we mentioned above, the effect of the entrance-channel mass-asymmetry was not evidently observed for the reactions leading to the non- (weakly-) fissile Yb and Hf compound nuclei with the fissility values

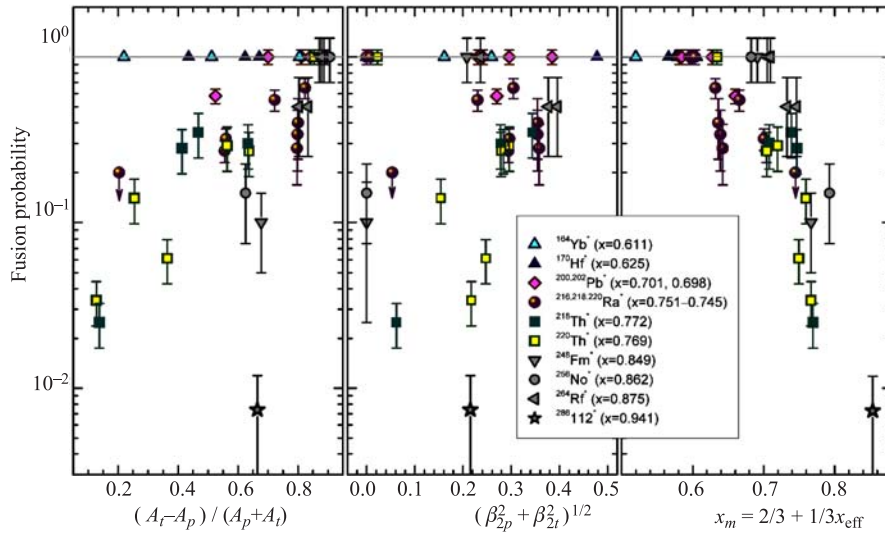


Fig. 9. The fusion probability (P_{CN}) values derived in the present analysis of the ER and fission excitation functions for reactions leading to the different compound nuclei (symbols) in the dependence on: 1) the entrance-channel mass-asymmetry (left panel); 2) the effective deformation in the entrance channel, which is expressed as a combination of the β_2 -values [16] for the projectile (p) and target (t) nuclei (middle panel); and 3) the mean arithmetic fissility proposed in the extra-push model [59] (right panel)

slightly above 0.6. One should note that according to the LD picture, the BG plateau is observed at the fissility value about 0.4 [12]. We see also that within this set of data the fusion suppression is observed in the reactions with the deformed partner(s) leading to the moderately fissile compound nuclei. For strongly fissile compound nuclei, fusion suppression is observed in asymmetric combinations with the spherical partners as well as with the deformed ones. We have also plotted the P_{CN} values as a function of the mean arithmetic fissility composed from the CN fissility and effective fissility taking into account Z and N of projectile and target nuclei, as proposed in the extra-push model [59] (see Fig. 9). It seems that it is possible to converge the data points with a proper choice of the weights in the sum for the mean arithmetic fissility, but even with this scaling,

it is clearly seen that the entrance-channel mass-asymmetry and fissility of a CN are the main parameters that determines the magnitude of the fusion suppression. The deformation of reactants affects fusion in reactions leading to the moderately fissile compound nuclei along with the entrance-channel mass-asymmetry.

In such data presentation, the fusion probability values corresponding to the reactions with the entrance-channel mass-asymmetry close to the BG point drop out of the visible systematic trend. One can remind that in [5] we obtained the same value of $P_{CN} = 0.65$ for $^{19}\text{F} + ^{197}\text{Au}$ corresponding to BG point as in [1], comparing their ^{19}F data with those obtained in $^{12}\text{C} + ^{204}\text{Pb}$ [1]. At the same time, our cross sections for ER produced in $^{12}\text{C} + ^{204}\text{Pb}$ at high excitation energies (see [5, 11] for details) are somewhat lower than those obtained in [1]. The joint fit to both the data gives us a smaller k_f -value. With this value, one can reproduce the ER cross sections for $^{19}\text{F} + ^{197}\text{Au}$ without any suppression of fusion [33]. To clarify the situation at the BG point we searched for the fusion suppression in the $^{18}\text{O} + ^{197}\text{Au}$ reaction, i. e., in the next-door neighbor with respect to $^{19}\text{F} + ^{197}\text{Au}$. The $^{197}\text{Au}(^{18}\text{O}, xn)$ excitation functions were recently measured in [60]. Our analysis of the ^9Be and ^{16}O excitation functions obtained in reactions leading to the $^{218,213}\text{Fr}^*$ compound nuclei and of those obtained in the ^{18}O -induced reaction leading to $^{215}\text{Fr}^*$ gave us the same LD-barriers ($k_f = 0.85$, assuming $P_{CN} = 1$). At the same time, for the ^{19}F reactions leading to the $^{217,213}\text{Fr}^*$ compound nuclei, independent fit to the measured ER and fission excitation functions [61] leads to the noticeably smaller LD barriers ($k_f = 0.78$) than those obtained previously. In order to use the barriers with $k_f = 0.85$ for the description of the ^{19}F data we should introduce phenomenologically $P_{CN} = 0.75$ [33]. This may be an indication that the fusion suppression really appears in going from ^{18}O to ^{19}F . Surely, it should be checked in experiments under the same conditions and for reactions leading to the same CN. The question on the nature of this suppression effect remains.

CONCLUSION

- Unexpected fusion suppression, which is connected with the quasi-fission effect and observed in quite asymmetric combinations of colliding nuclei, can be explained in the framework of the liquid drop model due to appearance of the conditional barrier along the mass-asymmetry coordinate on the path to the formation of a spherical compound nucleus.

- The fusion probability value as a measure of the fusion suppression correlates with the entrance-channel mass-asymmetry and fissility of a compound nucleus. The effect of fusion suppression is mainly inherent in reactions with deformed partners in cases of formation of the moderately fissile compound nuclei. In cases of reactions leading to strongly fissile compound nuclei, strong

fusion suppression is observed in reactions with deformed partners as well as in reactions with spherical ones.

• Attempts to search for a starting point of the fusion suppression, which can be associated with the Businaro–Gallone point, give us only indirect evidences for its decisive role in the appearance of the effect. Precise experiments performed under the same experimental conditions and exploring different mass-asymmetric combinations leading to the same CN are required.

REFERENCES

1. *Berriman A. C. et al. // Nature. 2001. V. 413. P. 144;*
Hinde D. J. et al. // J. Nucl. Radiochem. Sci. 2002. V. 3. P. 31.
2. *Back B. B. // Phys. Rev. C. 1985. V. 31. P. 2104.*
3. *Shen W. Q. et al. // Phys. Rev. C. 1987. V. 36. P. 115.*
4. *Chizhov A. Yu. et al. // Phys. Rev. C. 2003. V. 67. P. 011603.*
5. *Sagaidak R. N. et al. // Phys. Rev. C. 2003. V. 68. P. 014603.*
6. *Stefanini A. M. et al. // Eur. Phys. J. A. 2005. V. 23. P. 473.*
7. *Reisdorf W. et al. // Nucl. Phys. A. 1985. V. 438. P. 212.*
8. *Reisdorf W. // Z. Phys. A. 1981. V. 300. P. 227;*
Reisdorf W., Schädel M. // Z. Phys. A. 1992. V. 343. P. 47.
9. *Bass R. // Phys. Rev. Lett. 1977. V. 39. P. 265; Lect. Notes in Phys. 1980. V. 117. P. 281.*
10. *Cohen S., Plasil F., Swiatecki W. J. // Ann. of Phys. 1974. V. 82. P. 557.*
11. *Sagaidak R. N. et al. // Proc. of the 10th International Conference on Nuclear Reaction Mechanisms, Varenna, Italy, 2003. Milan, 2003. P. 301; JINR E7-2003-149. Dubna, 2003.*
12. *Davies K. T. R., Sierk A. J. // Phys. Rev. C. 1985. V. 31. P. 915.*
13. *Businaro U. L., Gallone S. // Nuovo Cimento. 1955. V. 1. P. 629; 1277.*
14. *Royer G., Remaud B. // Nucl. Phys. A. 1985. V. 444. P. 477;*
Royer G. et al. // Nucl. Phys. A. 1998. V. 634. P. 267.
15. *Moustabchir R., Royer G. // Nucl. Phys. A. 2001. V. 683. P. 266.*
16. *Möller P., Nix J. R., Myers W. D., Swiatecki W. J. // At. Data Nucl. Data Tables. 1995. V. 59. P. 185.*

17. Leigh J. R. *et al.* // Phys. Rev. C. 1995. V. 52. P. 3151.
18. Barreto J. L. *et al.* // Phys. Rev. C. 1993. V. 48. P. 2881.
19. Scarlassara F. *et al.* // Nucl. Phys. A. 2000. V. 672. P. 99.
20. Halbert M. L. *et al.* // Phys. Rev. C. 1989. V. 40. P. 2558.
21. Jiang C. L. *et al.* // Phys. Rev. C. 2005. V. 71. P. 044613.
22. Gil S. *et al.* // Phys. Rev. C. 1995. V. 51. P. 1336.
23. Charlop A. *et al.* // Phys. Rev. C. 1995. V. 51. P. 623.
24. Hinde D. J. *et al.* // Nucl. Phys. A. 1982. V. 385. P. 109.
25. Charity R. J. *et al.* // Nucl. Phys. A. 1986. V. 457. P. 441.
26. Bemis C. E., Jr. *et al.* ORNL Progress Report 1986 (ORNL-6326). P. 110.
27. Stefanini A. M. *et al.* // Eur. Phys. J. A. 2005. V. 23. P. 473.
28. Brinkmann K.-T. *et al.* // Phys. Rev. C. 1994. V. 50. P. 309.
29. Morton C. R. *et al.* // Phys. Rev. C. 1995. V. 52. P. 243.
30. Sagaidak R. N. *et al.* // Proc. of the VI International School-Seminar on Heavy Ion Physics, Dubna, Russia, 1997. Singapore, 1998. P. 323.
31. Morton C. R. *et al.* // Phys. Rev. C. 1999. V. 60. 044608.
32. Hinde D. J., Dasgupta M., Mukherjee A. // Phys. Rev. Lett. 2002. V. 89. P. 282701.
33. Sagaidak R. N. *et al.* // Proc. of the International Conference on Reaction Mechanisms and Nuclear Structure at the Coulomb Barrier, Venezia, Italy, 2006; AIP Conf. Proc. (in press).
34. Vermeulen D. *et al.* // Z. Phys. A. 1984. V. 318. P. 157.
35. Clerc H.-G. *et al.* // Nucl. Phys. A. 1984. V. 419. P. 571.
36. Stodel C. Thesis Ph.D. LPC-C T98-05. LPC Caen, 1998.
37. Morawek W. Thesis Ph.D. GSI report, GSI-91-26. 1991.
38. Mitsuoka S. *et al.* // Phys. Rev. C. 2002. V. 65. P. 054608.
39. Sahn C.-C. *et al.* // Nucl. Phys. A. 1985. V. 441. P. 316.
40. Hinde D. J. *et al.* // Phys. Rev. C. 1996. V. 53. P. 1290.
41. Akapiev G. N. *et al.* // At. Energ. 1966. V. 21. P. 243.

42. *Nishio K. et al.* JAERI Review, 2004-027. P. 39.
43. *Nurmi M. et al.* // Phys. Lett. B. 1967. V. 26. P. 78.
44. *Sikkeland T., Ghiorso A., Nurmi M.J.* // Phys. Rev. 1968. V. 172. P. 1232.
45. *Münzenberg G. et al.* // Z. Phys. A. 1981. V. 302. P. 7;
Heßberger F.P. et al. GSI Scientific Report 1986. GSI 87-1. 1987. P. 17.
46. *Keller H. et al.* // Z. Phys. A. 1987. V. 326. P. 313.
47. *Gäggeler H.W. et al.* // Nucl. Phys. A. 1989. V. 502. P. 561c.
48. *Yeremin A.V. et al.* // JINR Rapid Commun. 1998. No. 6[92]-98. P. 21.
49. *Oganessian Yu.Ts. et al.* // Phys. Rev. C. 2002. V. 65. P. 054602.
50. *Belozеров A.V. et al.* // Eur. Phys. J. A. 2003. V. 16. P. 447–456.
51. *Bock R. et al.* // Nucl. Phys. A. 1982. V. 388. P. 334.
52. *Pacheco A.J. et al.* // Phys. Rev. C. 1992. V. 45. P. 2861.
53. *Itkis M.G. et al.* // Proc. of the VI International Workshop on Fusion Dynamics at the Extremes, Dubna, Russia, 2000. Singapore, 2001. P. 93.
54. *Nitschke J.M. et al.* // Nucl. Phys. A. 1981. V. 352. P. 138.
55. *Somerville L.P. et al.* // Phys. Rev. C. 1985. V. 31. P. 1801.
56. *Lazarev Yu.A. et al.* // Phys. Rev. C. 2000. V. 62. P. 064307.
57. *Oganessian Yu.Ts. et al.* // Phys. Rev. C. 2004. V. 70. P. 064609.
58. *Oganessian Yu.Ts. et al.* // Phys. Rev. C. 2004. V. 69. P. 054607.
59. *Blocki J.P., Feldmeier H., Swiatecki W.J.* // Nucl. Phys. A. 1986. V. 459. P. 145.
60. *Corradi L. et al.* // Phys. Rev. C. 2005. V. 71. P. 014609.
61. *Mahata K. et al.* // Phys. Rev. C. 2002. V. 65. P. 034613.

Received on July 12, 2006.

Корректор *Т. Е. Понько*

Подписано в печать 27.09.2006.

Формат 60 × 90/16. Бумага офсетная. Печать офсетная.

Усл. печ. л. 1,18. Уч.-изд. л. 1,67. Тираж 310 экз. Заказ № 55490.

Издательский отдел Объединенного института ядерных исследований
141980, г. Дубна, Московская обл., ул. Жолио-Кюри, 6.

E-mail: publish@jinr.ru

www.jinr.ru/publish/